Mechanisms of Noncompetitive Inhibition of Acetylcholine-induced Single-Channel Currents

ROGER L. PAPKE and ROBERT E. OSWALD

From the Department of Pharmacology, College of Veterinary Medicine, Cornell University, Ithaca, New York 14853

ABSTRACT The functional mechanisms of noncompetitive blockade of the nicotinic acetylcholine receptor from the BC_3H-1 cell line were examined using single-channel currents recorded from cell-attached patches. Channel open times were distributed as sums of two exponentials and the closed times as sums of at least four exponentials. The single-channel currents of the receptor were analyzed in terms of activation schemes in which the receptor exists in two open states and a number of closed or blocked states. The existence of two distinct open states for the acetylcholine receptor allows for predictions to be made that will distinguish between different mechanisms of blockade. Notably, predictions could be made based on the model for the sequential block of open channels, that would allow us to discriminate such a mechanism, even for ligands that appear to dissociate so slowly that sequential openings of the same channel do not appear as distinct bursts. Four noncompetitive blockers of the acetylcholine receptor were studied: tetracaine, phencyclidine, and the (+) and (−) isomers of *N*-allylnormetazocine (SKF-10047). All four of these ligands decreased the duration of single-channel currents without increasing the number of fast closures per burst. The data suggest that the ligands block the channel in at least two distinct ways, one of which involves a specific interaction with open channels and the other is most consistent with the blockade of channels that may be either open or closed. In addition, the duration of the open state may be allosterically lengthened by the interaction of certain blockers with another class of sites.

INTRODUCTION

The nicotinic acetylcholine receptor (AChR) of the neuromuscular junction is a multisubunit protein with an integral ion channel. From enhanced electron microscopic images, the five subunits (α, β, γ, and δ with 2 α subunits per receptor) appear as a rosette with the ion channel in the center (Brisson and Unwin, 1985). The gating of currents through these channels depends on the presence of ligands, such as ACh, whose binding to specific sites on the α subunits leads to the opening of the channel.

Address reprint requests to Dr. Roger L. Papke, Molecular Neurobiology Laboratory, Salk Institute, 10010 North Torrey Pines Road, La Jolla, CA 92037.

J. GEN. PHYSIOL. © The Rockefeller University Press · 0022-1295/89/05/0785/27 $2.00
Volume 93 May 1989 785–811

Other types of ligands that bind to the receptor but do not cause activation fall into two broad categories: competitive antagonists, such as D-tubocurarine, that compete with ACh for the same sites but are ineffective at opening the channel, and noncompetitive blockers that affect function and bind to sites distinct from the agonist sites. The noncompetitive blockers constitute a heterogeneous group of ligands that have diverse effects on the function of the AChR (for review see Lambert et al., 1983), including effects on ion currents and the binding of other ligands. Effects of noncompetitive blockers can be observed on the macroscopic properties of receptors in membrane preparations and upon currents that flow through the individual receptors observed in patch-clamp experiments. Some of the effects of noncompetitive blockers include an increased rate of desensitization (Carp et al., 1983; Heidmann et al., 1983), shifts in the conformational equilibrium of the receptor (Changeux, 1981), a decrease in the apparent mean channel lifetime (Neher and Steinbach, 1978), and a decrease in the end plate current (EPC) decay time constant (Aguayo et al., 1981).

The diverse effects of these ligands could arise either from multiple sites on the receptor molecule for these agents or from effects on different conformational states of the receptor. In this regard, several studies have shown that agents such as phencyclidine, chlorpromazine, and several local anesthetics have a high affinity binding site as well as a larger number of low affinity, lipid-associated sites (Heidmann and Changeux, 1979; Cohen et al., 1980; Heidmann et al., 1983). Both the low and high affinity sites seem to be capable of modifying the conformational state of the receptor molecule and, in some cases, producing cooperative effects on changes in receptor conformational states (Sine and Taylor, 1982; Heidmann et al., 1983). The use of photoaffinity labels has suggested that the high affinity binding site may be near serine 262 of the δ subunit (Giraudat et al., 1986), with possible contributions from the other subunits (Oswald and Changeux, 1981; Cos et al., 1985).

The suggestion has been made that the high affinity site for these blockers is within the ion channel itself and that the inhibitor, upon binding, blocks the channel. In many, but not all, cases, the binding of noncompetitive blockers is enhanced by the rapid addition of agonist, which is consistent with the possibility that the ligands may have the highest affinity for the open state of the receptor. In the presence of blockers, such as the local anesthetic QX-222, the channels flicker rapidly between open and closed (or blocked) states (Neher and Steinbach, 1978). Kinetic analysis of such records supports a model for the sequential block of open channels, with the blocker specifically associating with the open state and with the channels restricted from going to the normal closed state while blocked. The total open time per burst remains constant but the duration of the burst lengthens in proportion to the time that the channel spends in the blocked state.

In the presence of a blocker such as QX-222, brief closures, which appear within bursts of current, and increase in frequency as a function of antagonist concentration, are associated with blocked states of the receptor. The gaps associated with channel blockade, however, can only be identified in single-channel records if the antagonist unbinds from the channel very rapidly, i.e., has a fast unblocking rate. In this paper, we describe in detail the effects of four different noncompetitive block-

ers that all appear to have relatively slow unblocking rates but which have different properties of binding to the AChR.

The noncompetitive blockers used in this study were: phencyclidine (PCP), tetracaine, and both the (+) and (−) isomers of *N*-allylnormetazocine (ANMC, SKF-10047). PCP was chosen because it exhibits a high selectivity for the site for noncompetitive blockers in binding studies and binds with tenfold higher affinity in the presence than in the absence of cholinergic agonists (Oswald et al., 1984). Tetracaine was used because, unlike PCP, it binds to the AChR with lower affinity in the presence than in the absence of agonists (Strnad and Cohen, 1983). Finally, the two isomers of *N*-allylnormetazocine interact both with the AChR and acetylcholinester-

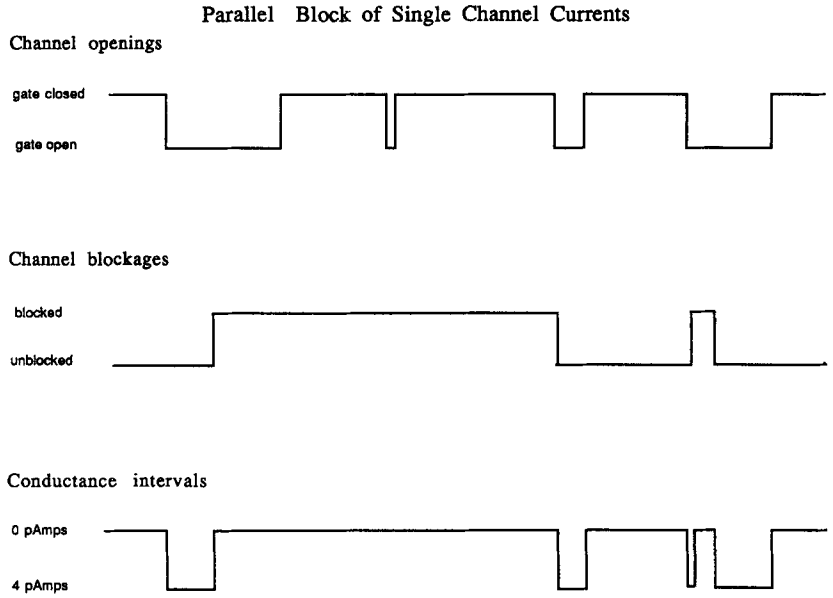

FIGURE 1. Model mechanism of parallel blockade of single-channel currents. The gating mechanism of the channel occurs independently of the binding of blocker as indicated in the upper trace. The binding of a blocking ligand is represented in the middle trace. The lower trace represents the time when the channel can carry current (conductance intervals), i.e., when the channel gate is open and no blocker is bound.

ase (Coleman et al., 1987) in a stereospecific manner (the (−) isomer is of two to threefold higher affinity than the (+) isomer). The binding of these isomers to the AChR is of relatively low affinity (4–15 μM) and the affinity is increased by less than twofold by carbamylcholine (Oswald et al., 1986). All four of these ligands decreased the duration of single-channel currents without an increase in the type of fast closures that would be observed with local anesthetics such as QX-222. Possible mechanisms for the decrease in the apparent duration of channel openings are considered in terms of the activation mechanism of the receptor, models for channel blockade, and possible allosteric interactions. We use the existence of two distinct open states of the receptor to test specific predictions of sequential block models.

An alternative model of parallel block is proposed that makes predictions that better fit the data for two of the ligands tested. A parallel block assumes that the blocker can associate with either the open or closed state of the receptor and that the binding of the blocker prevents the flow of current but still permits the conformational changes associated with gating of the channel. The single-channel currents observed represent times when the channel's gate is open and there is no blocker bound. We may refer to these events as conductance intervals. A conductance interval begins when either unblocked channels gate to the "open-gated state" or when channels that are in the "open-gated state" dissociate the blocker, see Fig. 1. The predictions of this model and that of the sequential blocking model are summarized in Table I for ligands with fast or slow dissociation rates.

We make two basic assumptions for the analysis presented. We assume that a ligand with a sequential blocking mechanism has a high affinity for the open state of

TABLE I

Predictions Based on Blocking Mechanisms

Mechanism	Off rate	Open times	Burst durations	A_s/A_f	New closed states
Sequential	Rapid	↓	↑	No effect	Yes
	Slow	↓	↓*	↑‡	Maybe§
Parallel	Rapid	↓	No effect‖	No effect¶	Yes**
	Slow	↓	↓	No effect	Maybe‡‡

*Since reopenings of blocked channels appear as separate bursts.

‡Slope of the increase determined by the ratio of the blocker's off rate to the normal frequency of channel activation.

§New component of the closed time distribution is present but may not be distinguished from other closed times.

‖Multiple openings of blocked channels may be resolved within bursts of normal duration.

¶A small increase in the percentage of long bursts may be indicated if openings appear to be in isolation.

**New closed times may appear and the number of such closures will be limited by the number of blockages that can be resolved within bursts of normal duration.

‡‡If the off rate of the blocker is much slower than the normal frequency of activation, prolonged closed times may appear.

the receptor, and that the affinity is the same for both long-lived or short-lived open states. A sequential mechanism implies a binding site within the channel itself, and the fact that the channel conductance is the same for both the brief and the long-lived open states implies that the conformation of the channel itself is the same in either open state. The second assumption is that the currents observed arise from a homogeneous population of receptors, especially in regards to their interactions with the ligands tested. Sine and Steinbach's (1986*b*, 1987) analysis of single-channel currents from the BC_3H-1 cell line provide good evidence for the brief and the long-lived open states arising from a single population of receptors.

MATERIALS AND METHODS

Tissue Culture

All experiments were conducted using BC_3H-1 cells obtained from American Cell Type Culture Association (Rockville, MD). Cells were grown and maintained in Dulbecco's Modified

Eagle's Medium with 10% fetal calf serum (without antibiotics) at 37°C in 10% CO_2 and passed weekly. After enzymatic dissociation of the stock cultures, an aliquot of cells was centrifuged, resuspended in growth medium, and plated on 35-mm dishes to be used for experiments. After 1 d, these cells were rinsed with a low serum medium (0.5% fetal calf serum) and subsequently maintained in low serum medium (Olsen et al., 1983). Cells were used for recording 8–18 d after the serum change with medium changes every 4–5 d.

Recording and Analysis of Single-Channel Records

All records were obtained at room temperature (22–24°C) using the cell-attached recording configuration (Hamill et al., 1981) with patch-clamp electronics (10-GΩ probe) (DAGAN Corp., Minneapolis, MN). A modified Ringer's solution consisting of 147 mM NaCl, 5.4 mM KCl, 1 mM $MgCl_2$, and 10 mM HEPES was used both in the bathing medium and inside the pipette (4.0 μM tetrodotoxin was included in the pipette). ACh and noncompetitive blockers, when included, were added to the pipette solution. Except where noted, the effects of noncompetitive blockers were tested in the presence of 100 nM ACh. When used, alpha-bungarotoxin (α-Bgt) was added to the cultures 30 min before the onset of recording. Experiments in the absence of ACh were performed with either an electrode holder never used with ACh or with a holder soaked for 24 h in 1-liter aliquots of distilled water with several solution changes.

Pipettes were constructed from borosilicate glass (TW 150-4; World Precision Instruments, Inc., New Haven, CT) and coated within 50 μm of the tip with Sylgard. The initial resistance of the fire-polished pipettes ranged from 4 to 8 MΩ. In the experiments done in the presence of highest concentration of PCP (20 μM), patches were very unstable and it was necessary to use pipettes that were not Sylgard coated. The use of uncoated pipettes gave more stable, although noisier, recordings. Therefore, the records obtained with uncoated pipettes were filtered at 2.5 kHz for analysis; all other records were filtered at 10 kHz using a Krohn-Hite filter (Avon, MA) and stored on FM tape. The data were digitized at an effective rate of 40 kHz using a PDP 11/24 computer (AR11 analog-to-digital converter). Using software written in assembly language, channels were detected by a simple threshold crossing algorithm with hysteresis (i.e., the displacement for determining an opening transition was the same as that for detecting a closing transition. In most cases, the threshold for an opening transition was 0.7 of the channel amplitude, and the threshold for the closing transition was 0.3 of the channel amplitude.) Then the channels were viewed on a monitor before inclusion in the analysis. The distributions of the open and closed events were analyzed on Micro VAX I and II computers (FORTRAN-77 programs developed in the laboratory) using the maximum likelihood criterion (Colquhoun and Sigworth, 1983) for convergence, fitting to one-, two-, three-, and four-exponential models with a Simplex algorithm (Caceci and Cacheris, 1984). In all cases, maximum likelihood fits were made to the individual durations. The minimum detectable event, given the characteristics of the amplifier, the filtration, and the analysis system, was found experimentally to be 50 μs. Using this value (t_{min}), the maximum likelihood fits were corrected as described by Colquhoun and Sigworth (1983). Values reported represent the means ± SEM for the fits of 3–12 (usually 5–8) records obtained under the same experimental conditions.

Burst analysis was conducted as described previously (Papke and Oswald, 1986; Papke et al., 1988) to define channel openings that occurred in groups of one or more (Sakmann et al., 1980). The time interval for defining a closure within a burst (t_c) was determined by systematically testing intervals between 0 and 20 ms and calculating the mean "burst duration" for one- and two-exponential models. The time constants for the burst duration distributions were then plotted as a function of the time interval. In all cases, the closures within a burst were much shorter than closures between bursts, so that the calculated time constants

reached a plateau. The time interval determining a closure within a burst was then defined as the first point after which the plateau occurred (typically 1 ms).

Unless otherwise stated, the data presented were obtained at a holding potential of 80 mV hyperpolarized from rest. The voltage dependence of burst duration was examined by recording at holding potentials between 120 and 60 mV hyperpolarized from rest, and between 80 and 120 mV depolarized from rest. Burst durations at voltages other than 80 mV hyperpolarized for each patch were then normalized to the value observed for that same patch at 80 mV hyperpolarized. In this way, the data obtained from multiple patches could be pooled for each experimental condition. Voltage dependencies can be described by their characteristic voltages, that is, the potential difference required to see an e-fold change under a given set of conditions. The greater the voltage dependence, the smaller the characteristic voltage, so that voltage dependence scales as the inverse of the characteristic voltage. To illustrate the relative voltage dependence of burst duration under various experimental conditions, data were normalized to the voltage dependence in the presence of 100 nM ACh alone and plotted as control characteristic voltage/characteristic voltage vs. ligand concentration.

RESULTS

Single-Channel Conductances

Control conditions. Three types of channels were repeatedly observed in these cells. In the presence of ACh, the vast majority of single-channel events could be attributed to an AChR channel of 50 ± 10 pS with a reversal potential of 20–30 mV depolarized from rest. Events of brief duration, $\tau = 0.5$ ms, and similar conductance were observed very rarely (no more than one per minute) in the absence of agonist and not at all in cells that had been previously exposed to α-Bgt, which suggests that they might represent extremely rare spontaneous openings of the AChR channel. In general, 50-pS events required the presence of agonist and in all cases were blocked by α-Bgt. Another channel that was observed in ~20% of the patches had a conductance of ~20 pS and a slightly more hyperpolarized reversal potential. These channels could be observed with equal probability after exposure to α-Bgt or in the absence of agonist and were, therefore, assumed not to be a class of AChR. This channel may be the same as the 27-pS nonselective cation channel described by Sheridan (1986). These currents were below the amplitude threshold for selection of events and so were excluded from the analysis. A third type of channel had an extremely low conductance, appearing as bursts of noise, and showed a reversal potential depolarized 50–70 mV from rest. Activity of this sort was inhibited by holding the patch at a depolarized potential for several seconds and then repolarizing the patch, or by including tetrodotoxin at relatively high concentrations (>1 μM). Only the 50-pS channel was studied in detail, and it is the channel referred to exclusively throughout the remainder of this paper. Under control conditions, the recordings represented stationary conditions, and the frequency of events did not change significantly ($P > 0.05$) during a record. Event frequency was tested by a regression analysis of burst frequency vs. time during a record. The slopes obtained were not significant and were equally positive and negative. Single-channel currents were ~5 pA at a holding potential 80 mV hyperpolarized from rest.

Effects of blockers. None of the ligands tested had a significant effect on the mean channel conductance. In both the presence and absence of these noncompeti-

tive inhibitors, the current-voltage relationships were linear in the range from 100 mV depolarized to 80 mV hyperpolarized relative to the resting potential, with a slope of 50 ± 0.5 pS. In some cases when recording in the presence of high concentrations of blocker (e.g., ≥5 μM PCP or ANMC), an increased activation of some of the low conductance channels was observed. This often made recording ACh currents difficult or impossible, particularly at depolarized potentials.

Open Times and Burst Durations

Openings of the channel occur as groups of one or more events, referred to as bursts. Due to the limited temporal resolution of the recordings and the analysis (t_{min} = 50 μs), some fast closures are not resolved and, therefore, the measured open times are overestimates of the actual duration of elementary open events. The complete closed time distribution, as fit by the maximum likelihood analysis, takes into account those events faster than t_{min} (Colquhoun and Sigworth, 1983) and indicated that only ~60% of all fast gaps (those longer than t_{min}) are directly detected, with multiple openings separated by fast gaps shorter than t_{min} appearing as single events. Burst analysis provides a method to describe the durations of groups of openings that is not biased by the presence of fast closures, since burst durations include both resolved and unresolved fast closures less than some minimum time t_c.

Considering closures <1 ms to be intraburst closures, the average number of openings per burst was less than two for all of the conditions tested (see Table III), i.e. even in the presence of blockers an average of less than one fast closure (<1 ms) per burst was observed. The number of fast closures per burst decreased in the presence of each of the blockers tested, and both open times and burst durations were shorter in the presence of blockers (see also the section on closed times). Since burst durations are more easily interpreted, the effects of the noncompetitive blockers are expressed in terms of burst durations.

Control observations. When recordings were made in the presence of ACh alone, the open times and burst durations could be fit with sums of two exponentials (Fig. 2). For open times the time constants were τ_1 = 0.20 ± 0.01 ms and τ_2 = 10.6 ± 1.0 ms, and for burst durations the constants were τ_{b1} = 0.21 ± 0.01 ms and τ_{b2} = 14.5 ± 1.7 ms (Fig. 3). Burst durations did not appear to be affected by agonist concentration. The ratio of slow to fast events (A_s/A_f), however, increased with increasing ACh concentration up to 2 μM (Fig. 3). The faster events represented 46 ± 3% of the burst distribution at 100 nM ACh, which was the concentration of agonist used in most experiments on the effects of noncompetitive blockers.

Effects of tetracaine. The effect of varying concentrations of tetracaine on the apparent elementary open time distributions and burst durations was studied at 0 and 100 nM ACh. Burst durations (t_c = 1.0 ms) at concentrations of tetracaine 10 μM and above were essentially identical to apparent open time distributions, suggesting that events occurred in isolation. Fig. 4 shows representative burst duration histograms obtained in the presence of 100 nM Ach and increasing concentrations of tetracaine. The most noticeable effect of tetracaine was to decrease the mean channel lifetime and burst duration for the slower exponential (IC_{50} of 5 μM). These results are summarized in Fig. 5 *A* which shows the dependence of the slower time constant on the tetracaine concentration in the presence of 100 nM ACh. Similar

results have been observed using the local anesthetic bupivacaine (Aracava et al., 1984). At concentrations of tetracaine near the IC_{50} (2–10 μM), open time and burst duration distributions were sums of two exponentials. Although τ_{b2} was decreased, the ratio of slow to fast openings remained the same as the control distribution.

At concentrations of tetracaine above 50 μM in the absence of ACh, 50-pS channel openings were observed that were more frequent than those observed in the absence of both ACh and tetracaine, confirming that tetracaine was capable of act-

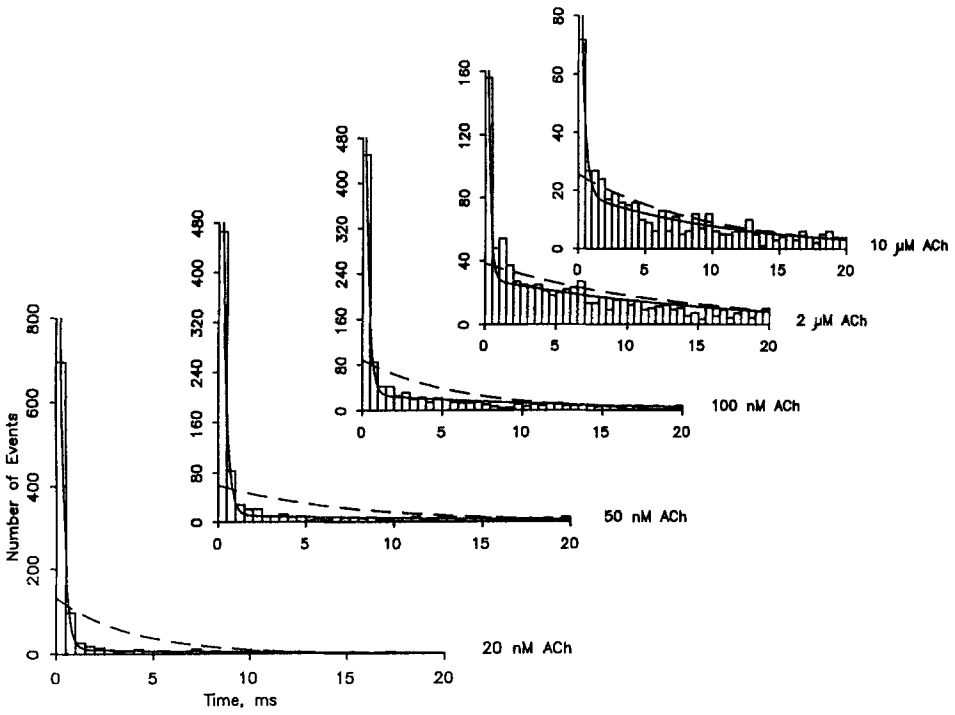

FIGURE 2. Burst time distributions obtained in the presence of different concentrations of ACh. The curves drawn through the bins represent the fit of the data generated by maximum likelihood analysis, fitting to either one (broken line) or two (solid line) exponential models. In each case, the data were obtained at a holding potential 80 mV hyperpolarized from rest. The number of observed events for each histogram were: 1,083, 20 nM; 909, 50 nM; 1,156, 100 nM; 1,010, 2 μM; 554, 10 μM.

ing as an agonist at these concentrations (see Papke and Oswald, 1986; note that at these concentrations tetracaine is capable of inhibiting the binding of $\alpha[^{125}I]$Bgt; Strnad and Cohen, 1983). The apparent elementary open time and burst duration distributions of tetracaine-induced openings were single exponentials with time constants of 0.25 ± 0.02 ms at 100 μM tetracaine, decreasing to 0.17 ± 0.01 ms at 200 μM tetracaine. These events were eliminated by pretreatment with α-Bgt.

Effects of ANMC. Both isomers of ANMC were effective in decreasing the duration of both fast and slow duration open times and bursts (see Fig. 6 for distribu-

tions observed in the presence of increasing concentrations of (−) ANMC). Most easily detected effects were on the duration of the slow component of the burst duration distributions, with an IC_{50} of ~1 μM for both isomers (1.2 ± 0.4 for (−)ANMC and 0.9 ± 0.2 for (+)ANMC; Fig. 7; at 1 μM the burst duration of the (+) isomer was not significantly different from control, $P > 0.2$). The block of fast events required higher concentrations. For both isomers, distributions would be well fit to the sum of two exponentials with concentrations of up to 10 μM. The ratios of slow and fast bursts were also affected by the presence of both isomers of

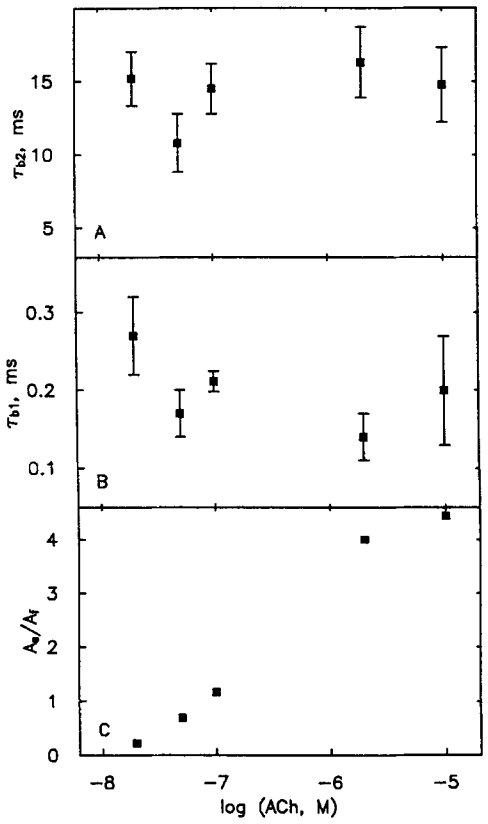

FIGURE 3. Parameters of the two exponential fits of the burst time durations obtained at different concentrations of ACh and a holding potential 80 mV hyperpolarized from rest. (*A*) The time constant of the slow component of the burst time distributions. (*B*) The time constant of the fast component of the burst time distributions. (*C*) The ratio of the area contributed by the slow component of the burst time distributions to that of the fast component, at different concentrations of ACh. The number of patches averaged for each point are (from left to right in increasing ACh concentration) 6, 5, 11, 4, and 3.

ANMC, with the relative numbers of slow duration events increasing with higher concentrations of either isomer.

Effects of PCP. Single-channel currents were recorded in the presence of 100 nM ACh and concentrations of PCP ranging from 10 to 20 μM. As previously reported (Papke and Oswald, 1986), concentrations of PCP > 1 μM decreased channel open time, with no significant effect at 1 μM PCP. In these experiments, however, effects of PCP were observed both at concentrations > 1 μM and ≤ 500 nM. Representative burst duration histograms obtained in the presence of increasing concentrations of PCP are shown in Fig. 8. Fig. 9, *A* and *B* shows the effect of PCP on the duration of the slower and faster components of the burst duration distribu-

tion. Significant decreases in burst duration were observed at concentrations of 100 ($P < 0.05$) and 500 nM PCP ($P < 0.05$) as well as concentration ≥ 2 μM ($P < 0.001$). At 100 nM PCP, burst duration is decreased to 9.4 ± .6 ms from the control value of 14.5 ± 1.7. The relative percentage of slow bursts was also increased in the presence of >2 μM PCP.

The effects of the blockers on open times, burst durations, and the ratios of slow and fast bursts (A_s/A_f) are summarized in Table II. Plots of reciprocal burst duration vs. antagonist concentration were linear for (−)ANMC, tetracaine, and PCP at

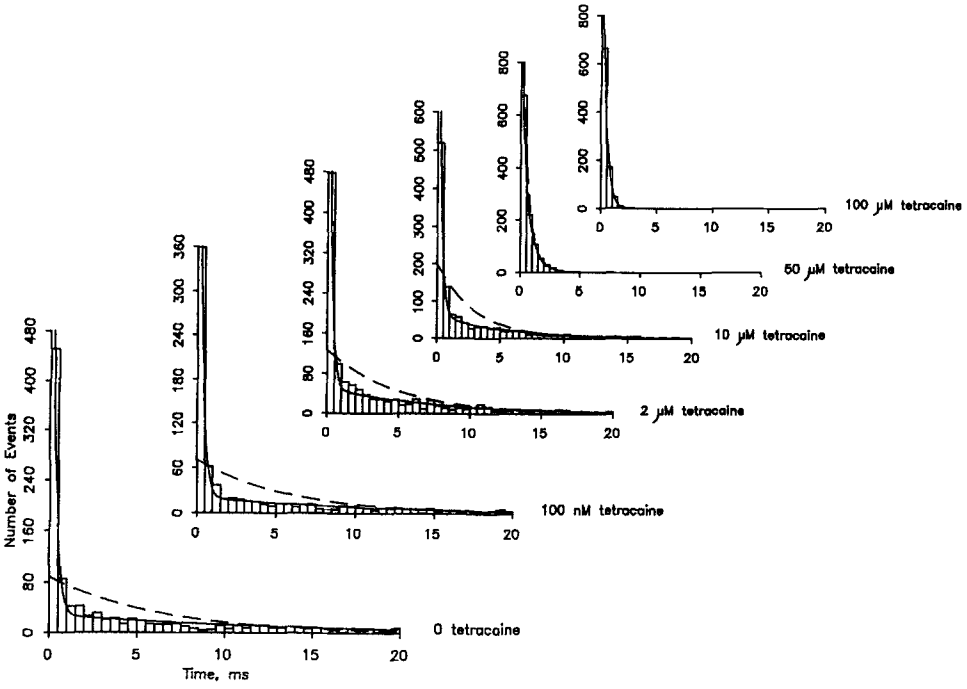

FIGURE 4. Burst time distributions obtained in the presence of 100 nM ACh and different concentrations of tetracaine. The curves drawn through the bins represent the fit of the data generated by maximum likelihood analysis, fitting to either one (broken line) or two (solid line) exponential models. In each case, the data were obtained at a holding patential 80 mV hyperpolarized from rest. The number of observed events from each histogram were: 1,156, 0 nM; 826, 100 nM; 1,279; 2 μM; 1,205, 10 μM; 1,114, 50 μM; 900, 100 μM.

the concentrations 1 μM and greater ($r^2 > 0.99$, r^2 for (+)ANMC = 0.881, data not shown), while this relationship was nonlinear at low concentrations (<1 μM) of PCP and (+)ANMC.

Closed Time Distributions

Control observations. In the presence of ACh alone at concentrations <1 μM, closed time distributions were fit by four exponentials. A representative histogram is displayed in Fig. 10 *a*. The bin width is plotted on a logarithmic scale (Sigworth and

Sine, 1987). With such a plot, the maxima occur at the time constant for each exponential component. Two relatively fast components were observed: τ_{c1} = 0.041 ± 0.003 ms and τ_{c2} = 0.57 ± 0.12 ms, making up 29 ± 7% and 5.3 ± 0.6% of the distributions, respectively. A third component can also be observed (τ_{c3} = 5.0 ± 0.75 ms at 100 nM ACh), making up <3% of the total distribution. The predominant slow closed times (τ_{c4} = 120 ± 60 ms, in the presence of 100 nM ACh alone) were highly variable presumably corresponding to variations in the numbers of channels in a patch.

To estimate the effect of channel blockers on the closing rates of the channel, the

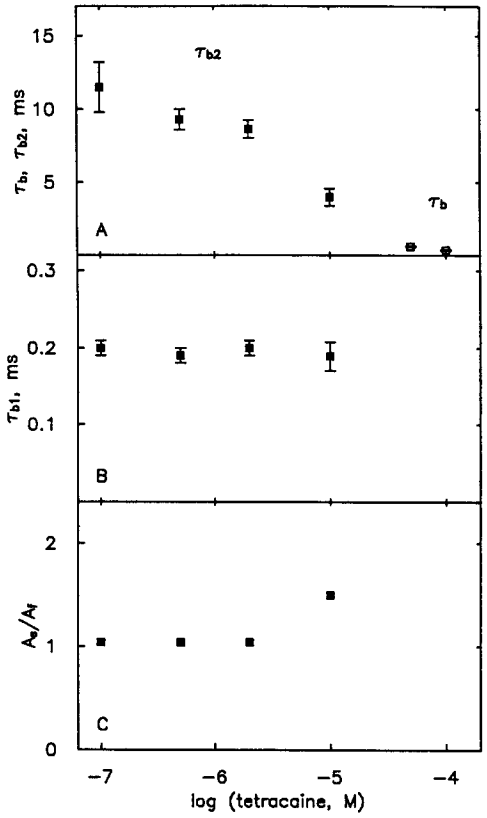

FIGURE 5. Parameters of the burst time durations obtained in the presence of 100 nM ACh and different concentrations of tetracaine. (*A*) The time constant of the slow component of the burst time distributions is plotted for concentrations of tetracaine <50 μM. At concentrations greater than or equal to 50 μM tetracaine, burst durations no longer fit two exponentials so that the points plotted for the highest two concentrations represent the single exponential fits (τ_b). (*B*) The time constant of the fast component of the burst time distributions. (*C*) The ratio of the area contributed by the slow component of the burst time distributions to that of the fast component, at the different concentrations of tetracaine. The number of patches averaged for each point are (from left to right in increasing tetracaine concentration) 6, 7, 4, 7, 3, and 7.

frequency of fast closures was calculated from the total numbers of τ_{c1} and τ_{c2} closures and the total time spent in the open time. Such an estimate of the closing rate is less biased than one based on the apparent open times because it takes into account missed closures by using the reconstructed portions of the closed time distributions less than t_{min} (Papke et al., 1988). For 100 nM ACh alone, the fast closures occurred at a rate of 54 s^{-1} for time spent in either of the open states (see Table III). An increase in the frequency of such fast closures in the presence of blockers would suggest either an increase in the intrinsic closing rate(s) or the introduction of new fast closed (i.e., blocked) states.

Effects of tetracaine. The closed time distribution in the presence of tetracaine indicated a decrease in the percentage of fast closures (<1 ms) with increasing tetracaine concentration (see Fig. 10 *b*). Components exhibiting a time constant of <1 ms (i.e., τ_{c1} and τ_{c2} closures) decreased from 30 ± 6% in the absence of tetracaine to 6.8 ± 4% at 100 μM tetracaine and 100 nM ACh. The loss of the fast closures indicates that the events observed in the presence of tetracaine are isolated events, consistent with the near identity of the elementary open time and burst duration distri-

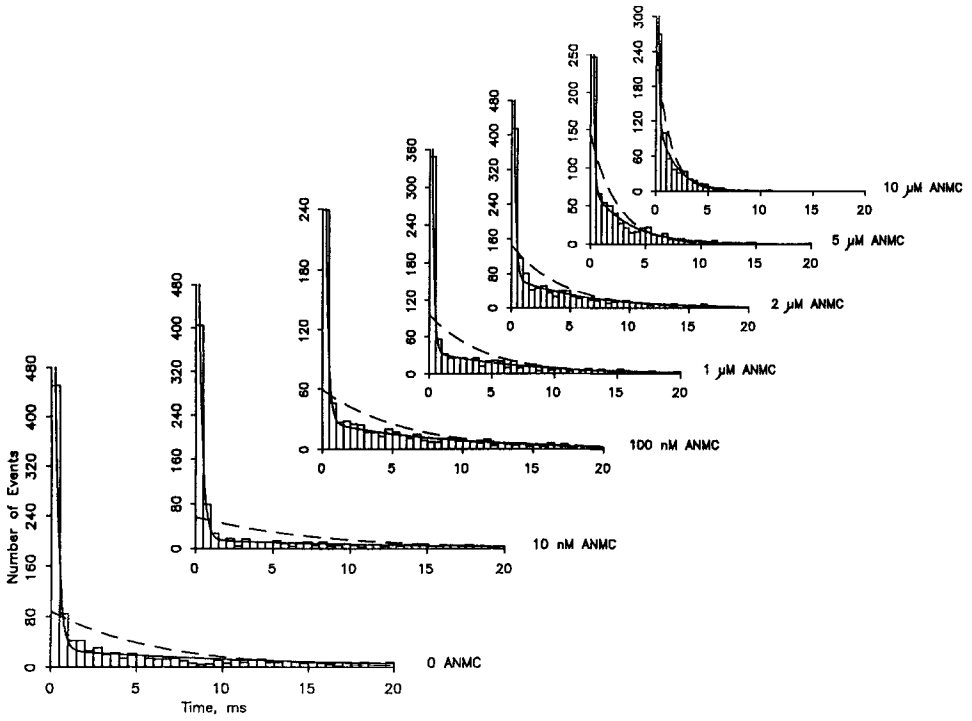

FIGURE 6. Burst time distributions obtained in the presence of 100 nM ACh and different concentrations of the (−) isomer of ANMC. The curves drawn through the bins represent the fit of the data generated by maximum likelihood analysis, fitting to either one (broken line) or two (solid line) exponential models. In each case, the data were obtained at a holding potential 80 mV hyperpolarized from rest. The number of observed events for each histogram were: 1,156, 0 nM; 925, 10 nM; 705, 100 nM; 838, 1 μM; 1,243, 2 μM; 673, 5 μM; 616, 10 μM.

butions. The frequency of fast closures, however, in the presence of tetracaine actually increases somewhat (see Table III) but only at concentrations above the IC_{50} for the block of show events. Furthermore, with increasing concentrations of tetracaine, the predominant fast closed state was represented by the time constant of τ_{c2} closures (0.6 ms), and the number of τ_{c1} type closures became very small.

Effects of ANMC. Closed time distributions in the presence of ANMC were also fit by four exponentials. Two fast components were observed that did not vary in duration and decreased in their relative number (see Table III) with increasing con-

centrations of ANMC. The (−) isomer, but not the (+) isomer, showed a greatly increased rate of fast closures at concentrations above the IC_{50} for the block of slow events (see Table III).

Additionally, in the presence of increasing concentrations of (+) or (−) ANMC, an increasing number of events are fit by an intermediate component of longer duration than the τ_{c3} component observed in controls (Fig. 10 *C*). At concentrations ≥ 1 μM, τ_{c3} was 11.8 ± 1.3 ms for the (−) isomer and 14.6 ± 1.6 ms for the (+)isomer, representing 20–30% of the closed times at concentrations >2 μM of either isomer. The relative number of these events increased with the concentration

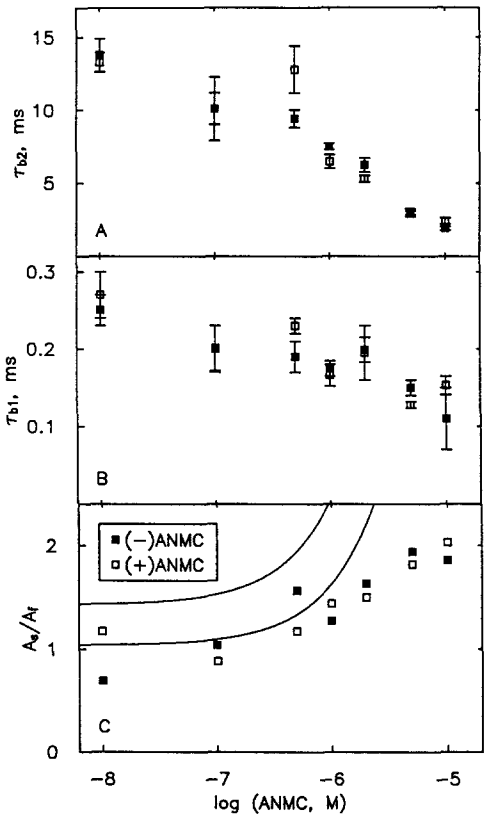

FIGURE 7. Parameters of the two exponential fits of the burst time durations obtained in the presence of 100 nM ACh and different concentrations of (+) and (−)ANMC. (*A*) The time constant of the slow component of the burst time distribution. (*B*) The time constant of the fast component of the burst time distributions. (*C*) The ratio of the area contributed by the slow component of the burst time distributions to that of the fast component, at the different concentrations of ANMC. The smooth curves were generated as described in the Appendix and represents the range of values of A_s/A_f at each concentration that would be consistent with a simple sequential model given the experimental error of the measurements. The number of patches averaged for each point are (from left to right in increasing ANMC concentration) 3, 5, 4, 4, 3, 4, and 4 for (+)ANMC; and 3, 3, 3, 3, 5, 4, and 7 for (−)ANMC.

of ANMC up to 2 μM of either isomer and showed no further increase at higher concentrations. τ_{c3} closures may represent time when the channel is blocked by the ligand, and from the duration of these closures, unblocking rates (k_{-b}) of 85 s^{-1} for the (−) isomer and 69 s^{-1} for the (+) isomer were calculated.

The existence of a component of the closed time distribution associated with the presence of ANMC suggested that some of the openings observed in the presence of ANMC might exist as bursts of openings separated by τ_{c3} closures. To define these bursts, a modified form of burst analysis was performed. Using records in which the time constants of the intermediate and long components of the closed time distribution (τ_{c3} and τ_4, respectively) were well separated (by greater than a

factor of 10) and a time threshold (t_c) of 30 ms, burst duration histograms were constructed that represented the durations of groups of openings that were separated by closed times <30 ms. The distributions thus constructed were compared with control records analyzed in the same fashion. The control records had only a small portion of closed times fit by a τ_{c3} component of shorter durations, and burst frequencies were similar.

Since such analyses of records obtained in the presence of ANMC created a new

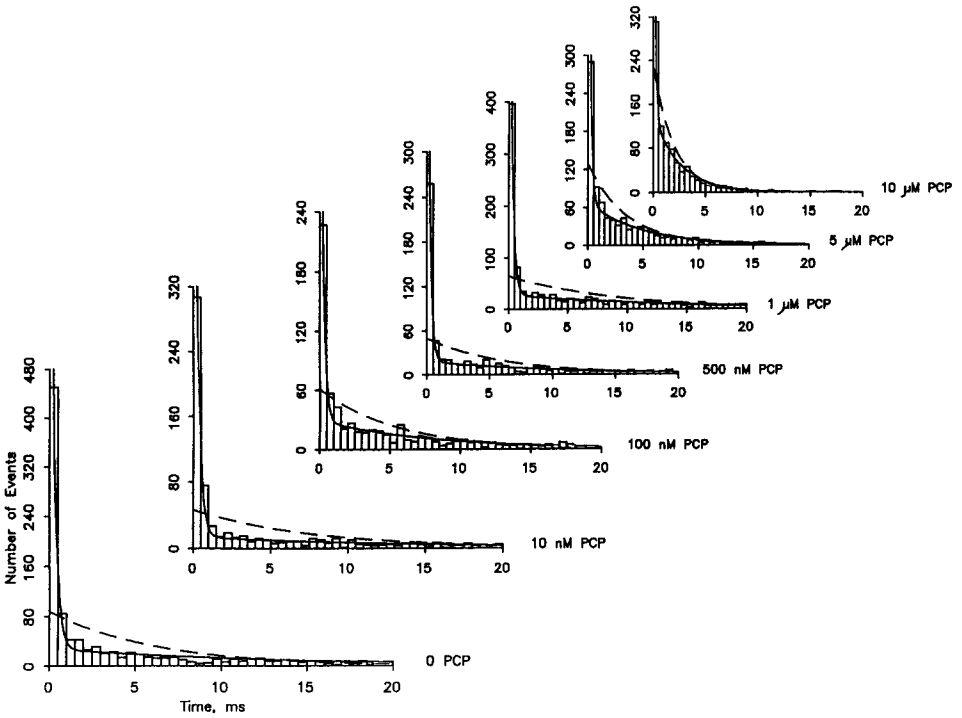

FIGURE 8. Burst time distributions obtained in the presence of 100 nM ACh and different concentrations of PCP. The curves drawn through the bins represent the fit of the data generated by maximum likelihood analysis, fitting to either one (broken line) or two (solid line) exponential models. In each case, the data were obtained with Sylgard-coated pipettes at a holding potential 80 mV hyperpolarized from rest. The number of observed events for each histogram were: 1,156, 0 nM; 755, 10 nM; 699, 100 nM; 645, 500 nM; 1,187, 1 μM; 905, 5 μM; 900, 10 μM.

type of longer burst, distributions contained three exponential components, with a new long component representing bursts in which closed times of intermediate duration had occurred (as well as the presumably random concatenation of a few other adjacent bursts). The histograms generated in this way from control data, however, were only slightly changed from these generated with the normal burst criteria of 1.0 ms, with no significant change in the time constant of the long bursts. The three-exponential fit of control data (with t_c = 30 ms) gave a τ_{b1} = 0.165 ± 0.005 ms, τ_{b2} = 2.5 ± 0.3 ms and τ_{b3} = 16.5 ± 1.5 ms, representing 37.5 ± 0.5, 12 ±

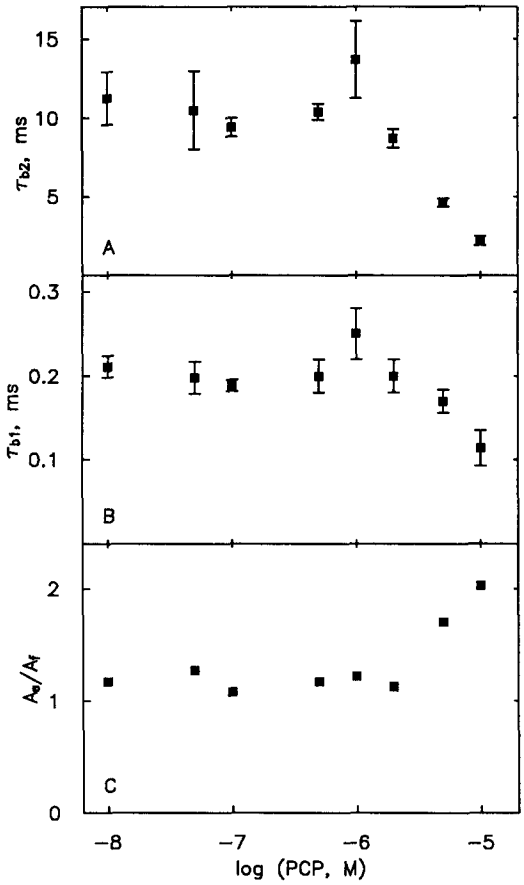

FIGURE 9. Parameters of the two exponential fits of the burst time durations obtained with Sylgard-coated pipettes in the presence of 100 nM ACh and different concentrations of PCP. (*A*) The time constant of the slow component of the burst time distributions. (*B*) The time constant of the fast component of the burst time distributions. (*C*) The ratio of the area contributed by the slow component of the burst time distributions to that of the fast component at the different concentrations of PCP. The number of patches averaged for each point are (from left ro right in increasing PCP concentration) 5, 5, 6, 5, 6, 7, 3, and 4.

1, and 50.5 ± 0.8% of the distribution, respectively. When the data obtained in the presence of ANMC were examined this way, 30.7 ± 2.6% was fit to the prolonged component, and the duration of this component (τ_{b3} = 15.0 ± 1.0 ms with ≥ 2 μM (−)ANMC) was not different from control burst durations (with t_c either 1.0 ms or 30 ms (τ = 14.5 ± 1.7 or 16.5 ± 1.5 ms, respectively). This suggests that the τ_{c3} closed times observed in the presence of ANMC represent blockages within bursts of normal duration, i.e., that bursts are not prolonged. The τ_{b2} component represents events isolated from other conductance intervals, more events were fit to the

TABLE II

Summary of Blocking Properties

Antagonist	Burst durations	A_s/A_f	Long closed states
Tetracaine	↓	No effect	No effect
PCP	↓*	↑	↑
(−)ANMC	↓	↑	New closed time (15 ms)
(+)ANMC	↓	↑	New closed time (12 ms)

*At concentrations less than and greater than 1 μM.

τ_{b2} at higher concentrations of ligand, and the τ_{b2} fit to these events decreased as a function of ANMC concentration. Similar analysis obtained with tetracaine (which seems to have an unblocking rate slower than the channel's closing rate) produced histograms with few events (≤5%) fit to a τ_{b3} component of variable duration, and not related to normal burst length, implying that closures within bursts are not resolvable with tetracaine due to the slow dissociation rate.

If the τ_{c3} closures do represent time that the channel is blocked, then after such a closure the channel might be expected to return to the same open state. To test this,

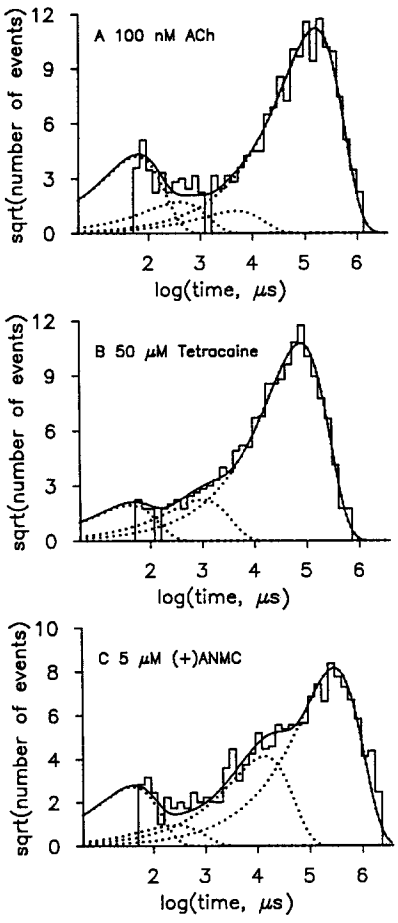

FIGURE 10. Closed time distributions obtained in the presence of (*A*) 100 nM ACh alone, (*B*) 100 nM ACh plus 50 μM tetracaine, and (*C*) 100 nM ACh plus 10 μM (+)ANMC. The bin size is based on a log time scale. With such a plot the various components can be visualized together and the time constants occur at peaks in the distribution. The solid curve through the data represents the four exponential fit obtained by maximum likelihood analysis (three exponential fit in the case of tetracaine) and the dotted lines represent the exponential components to the fit. The major components in the control distribution are the shortest and the longest closed times. In the presence of tetracaine, the relative numbers of brief closures are much fewer. In the presence of ANMC, the intermediate component, τ_{c3} ~ 14 ms, appears as a distinct shoulder on the peak associated with the longest closed times. All closed times including gaps between bursts are shown.

a correlation analysis (Jackson et al., 1983, Sine and Steinbach, 1986b) was conducted to determine whether closures fit to this time constant occurred randomly between either the faster or slower openings or preferentially between slower openings. Closed times were identified as τ_{c3} closures and openings were judged as being either fast or slow with the expected values corrected for misclassifications and the loss of events through the limited temporal resolution. χ^2 analysis then rejected the hypothesis ($P < 0.01$) that the closures occurred at random between openings, indicating rather that they occurred preferentially between pairs of the slow openings.

Effects of PCP. PCP had no significant effect on the time constants of the closed time distribution at concentrations <1 μM. Above 1 μM, a very long component of the closed time distribution was observed, which may represent either very long periods of blockade or increased equilibrium desensitization. When fit to a four-exponential distribution, the longest time constant (τ_{c4}) was on the order of several seconds and increased with increasing concentration of PCP (data obtained with uncoated pipettes, see also Papke and Oswald, 1986). The value of the next longest time constant was similar to the longest time constant observed in control distributions (τ_{c3} = 54 ± 20 ms in the presence of 10 μM PCP; τ_{c4} = 120 ± 60 ms, in controls), and the area represented by this component decreased with increasing PCP concentration.

The relative number of fast closures in the closed time distributions also decreases in the presence of PCP (see Table III); however, a small increase in the frequency of

TABLE III

Frequency of Fast Closures

Condition	Concentration	τ_o	num(τ_{c1} + τ_{c2})	Frequency (fast closures)
	μM	*ms*		
ACh alone	0.1	6.4	0.340	54.0
Tetracaine	2.0	4.15	0.277	66.8
	10	2.53	0.243	96.0
PCP	2.0	4.49	0.190	42.3
	5.0	2.78	0.270	97.0
(−)ANMC	2.0	3.66	0.197	42.3
	5.0	1.89	0.230	121.0
	10	1.09	0.330	302.0
(+)ANMC	2.0	3.15	0.147	46.7
	5.0	1.92	0.123	64.0
	10	1.71	0.107	62.5

The single exponential fit of the open time distribution (τ_o) represents the mean channel open time of both the slow and fast events. The (τ_{c1} + τ_{c2}) or number of fast closures per burst, gives the number of closures fit to either τ_{c1} + τ_{c2} per opening of the channel. The frequency of such closures is then the number per opening divided by the average open time in seconds.

fast closures is observed at high concentrations, above the IC_{50} for the block of slow events.

The effects of the blockers on long-lived closed times (>1 ms) are summarized in Table II, and effects of the blockers on the frequency of brief closed times are indicated in Table III.

Voltage Dependence

Control observations. In the presence of 100 nM ACh, burst duration increased with increasing hyperpolarization, having a characteristic voltage of 126 ± 10 mV. The effect of voltage on burst duration was greatest in the presence of low concentrations of agonist (see Fig. 11 *A*). The frequency of bursts was also influenced by voltage as well as the concentration of agonist. At low concentrations of agonist,

bursts were more frequent at hyperpolarized potentials. At higher concentrations of agonist, the burst frequency became less sensitive to voltage, and at concentrations of ACh > 1 μM, bursts were more frequent at depolarized potentials (Fig. 11 *B*). In the presence of 20 nM ACh, an *e*-fold increase in burst frequency would require 175 ± 20 mV hyperpolarization. In the presence of 100 nM ACh, the characteristic voltage was 320 ± 57 mV.

Effect of tetracaine. The voltage dependency of burst durations (τ_b or τ_{b2}) was modified markedly by tetracaine (Fig. 11 *C*). In the presence of tetracaine, the voltage dependency decreased and reversed at high concentrations (≥50 μM), indicating that the blockade is enhanced by hyperpolarization. The effect of tetracaine acting as an agonist at 100 μM (in the absence of ACh) shows similar voltage dependence of mean burst durations as ACh at 10 nM (data not shown).

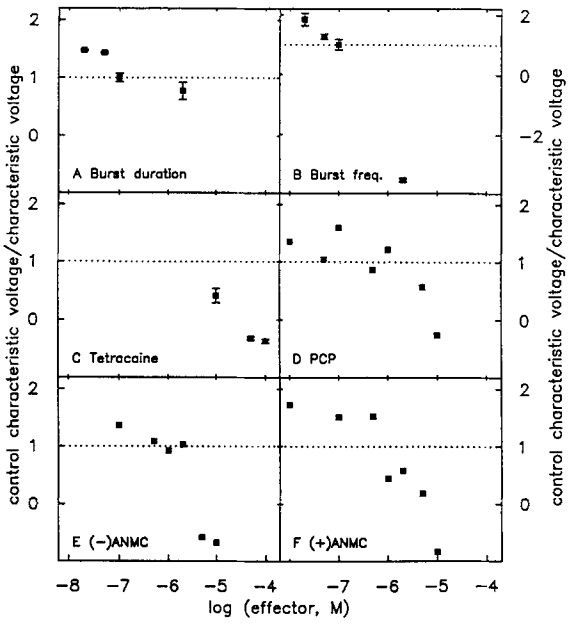

FIGURE 11. (*A*) The voltage dependence of burst duration as affected by the concentrations of ACh. (*B*) The voltage dependence of burst frequency as affected by the concentrations of ACh. (*C–F*) The voltage dependence of burst duration as affected by the concentrations of blocker: (*C*) tetracaine, (*D*) PCP, (*E*) (−)ANMC. The voltage dependence can be expressed as 1/characteristic voltage (see Methods), and the values shown have been normalized to the voltage dependence observed in the presence of 100 nM ACh alone. A value >1 indicates a smaller characteristic voltage, i.e., a greater effect of voltage; values below 0 reflect effects of voltage in the opposite direction of the control condition, i.e., burst durations are prolonged at more depolarized potential, rather than at more hyperpolarized potentials.

Effects of ANMC. The voltage dependence of burst duration (Fig 11, *E* and *F*) was decreased by concentrations >1 μM of either isomers and reversed at higher concentrations. At low concentrations (<1 μM) of the (+)isomer, the normal voltage dependence of burst duration also appears to be enhanced.

Effect of PCP. Fig. 11 *D* shows the effect of increasing the concentration of PCP on the voltage dependence of burst duration. PCP antagonizes the normal volt-

age dependence of burst duration only in the high concentration range of PCP's effects. At 100 nM PCP, the voltage dependence of burst duration is enhanced (i.e., exhibits a smaller characteristic voltage). At concentrations >1 μM PCP, the voltage dependence of burst duration decreases, and at ≥10 μM PCP, the voltage dependence is the opposite of the control and events are longer at the more depolarized potentials.

DISCUSSION

Single-channel currents of BC_3H-1 nicotinic AChRs have been described, and the effects of four noncompetitive ligands have been examined. The following observations were made: (*a*) In the presence of ACh alone, apparent open time and burst duration distributions were sums of two exponentials, with the percentage of slower openings increasing with increasing concentration. Closed time distributions in the presence of ACh (<1 μM) alone were fit by the sum of four exponentials. (*b*) The noncompetitive blockers had no effect on the single-channel conductance (tetracaine also acts as an agonist at concentrations >50 μM) but decreased both the apparent mean channel lifetime and mean burst durations at concentrations above 1 μM. A second range of effective concentrations for PCP existed in the nanomolar range, with no effect of 1 μM PCP, suggesting that the mechanism of PCP's effects may be complex. The effects of PCP and ANMC on the distribution of burst durations differ from that of tetracaine in that, with increasing concentrations of PCP and ANMC, the relative number of bursts fit to the slow component of the distribution increases, an effect that was not observed with tetracaine (see Table II for summary).

(*c*) The closed time distribution was uniquely affected by each of the noncompetitive blockers, although, in general, the presence of these noncompetitive blockers decreased the relative number of fast closures, so that the number of fast closures per burst was less than that which was observed in controls. The decrease in the number of fast closures per burst indicates that these ligands all had fairly slow unbinding rates at their primary blocking sites. At high concentrations, however, some of the ligands did show an increase in the frequency of fast closures, indicating that another form of channel block with a faster unbinding rate may also exist. In summary, tetracaine's only apparent effect on closed times was to decrease the relative number of fast closures; PCP seemed to prolong the longest closed time as well as to reduce the relative number of fast closures, and ANMC introduced a new component into the distributions. Detailed examination of records obtained in the presence of ANMC suggests that the class of closures associated with ANMC and fit to a τ_{c3} of ~14 ms are blocked periods within bursts of normal duration.

(*d*) In the presence of agonist alone, burst durations were longer and more frequent at more hyperpolarized potentials and low concentrations of agonist. The normal voltage dependence (especially of the frequency of bursts) was lower at higher concentrations of agonist. In general, the voltage dependency of burst duration was decreased in the presence of noncompetitive blockers.

Double exponential apparent elementary open time and burst duration distributions have been observed for most AChR channels that have been studied. Several groups have also reported that the percentage of slow openings increases with

increasing agonist concentration (Takeda and Trautmann, 1984; Colquhoun and Sakmann, 1985; Labarca et al., 1985; Papke and Oswald, 1986). Studying the BC_3H-1 cell AChR at 11°C, Sine and Steinbach (1984, 1986*a*, *b*) reported that the ratio of fast to slow openings did not vary as a function of agonists concentration; however, working at room temperature, Covarrubias and Steinbach (J. H. Steinbach, personal communication) have recently observed an effect of agonist concentration on the expression of the slow open state. The effect of agonist concentration of the relative expression of the two open states has led to the suggestion (Colquhoun and Sakmann, 1985; Labarca et al., 1985) that some of the fast events may represent the opening of singly liganded channels, as indicated in Scheme 1 below, where R is the unliganded closed channel, A represents the agonist, AR is a single liganded closed channel, A_2R is a doubly liganded closed channel, AR^* is a single liganded open channel, and A_2R^* is the doubly liganded open channel. This is the basic mechanisms to which we will relate the effects of noncompetitive blockers.

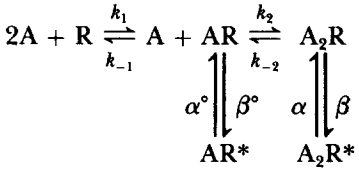

(Scheme 1)

The effects of noncompetitive inhibitors on open times have been described for many types of agents (for review see Changeaux, 1981) from alcohols (Gage et al., 1975; Gage, 1976) to local anesthetics such as QX-222 (Neher and Steinbach, 1978; Neher, 1983). The interaction of most of these agents with the AChR is influenced by the presence or absence of agonist. Most bind with greatest affinity in the presence of agonist (one exception being tetracaine), and many of the early studies of end-plate currents and single-channel currents suggested specific interactions with the open state of the receptor. A number of these studies were consistent with a sequential model for the block of open channels (see Scheme 2, below; ARB and A_2RB represent blocked states). For some substances such as QX-222 (Neher and Steinbach, 1978), the model seemed to fit well, at least within a limited concentration range (Neher, 1983). Channel openings were observed as bursts of current, with the channel flickering back and forth between open and blocked states. The fact that these bursts seemed to contain the same amount of total open time as normal bursts suggested a model that restricted binding of the noncompetitive blockers to open channels and required the channel to be in an unblocked state before the channel could close and the agonist could dissociate.

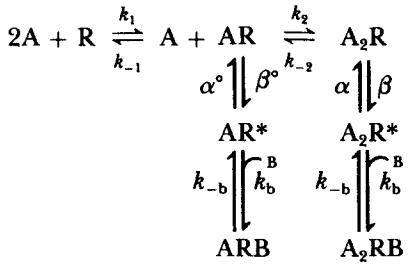

(Scheme 2)

The fact that some of these predictions are not satisfied either at high concentrations of certain agents (Neher, 1983), or not at all by others such as histrionicotoxin (Spivak et al., 1982), suggests that mechanisms other than sequential channel blockade may exist. The utility of the model, in general, has been limited by the fact that such effects are only clearly observable when the unblocking rate is relatively fast. The unblocking rates that have been attributed to ligands asserted to be sequential blockers have been much faster than the channel closing rates. In the present study, the effects of the four agents suggest that their unblocking rates are at least several orders of magnitude slower than that of a ligand like QX-222. However, by observing the differential effects on the two open states of the channel, results can still be compared with the predictions of the sequential model.

A simple sequential model (Scheme 2) of channel blockade predicts that the burst length (bursts in this case defined as the time during which a channel makes transitions between the open, blocked, and fast closed states before returning to the normal long closed state, see Table I) should increase with increasing blocker concentration and that the average total open time within a burst should be the same in the absence and presence of blocker (Neher and Steinbach, 1978; Colquhoun and Hawkes, 1983). Also, Scheme 2 predicts that an additional component of the closed time distribution should appear with a time constant equal to the reciprocal of the unblocking rate ($1/k_{-b}$). If one assumes that the unblocking rate (k_{-b}) is slow and of the same order of magnitude as the apparent opening rate constant (note that this is an apparent opening rate that can be influenced by desensitization, ACh binding, and the number of channels in the patch), a simple sequential block model would predict a decrease in the percentage of fast closures and a relatively unchanged time constant for the long closed times. The open time and burst duration distributions would show a decrease in τ_2 (or τ_{b2}) and an increase in the percentage of events fit to the slower component of the distributions. The reason for this is that a sequential block model predicts that the longer a channel is open, the greater the chance it will interact with the blocker and pass to the blocked state. The result is a preferential effect on the longer-lived open state and an apparent increase in the number of events of this type, which exhibit a shortened time constant (equal to $1/[\alpha + xk_b]$, where $1/\alpha$ is the normal burst duration, x is the concentration of blocker, and k_b is the forward binding constant to the open form of the receptor). Passage of a blocked channel back to the open state is recorded as another event with the same mean open channel lifetime as the previous event. Thus, this increase in the number of events occurs selectively for open states with long lifetimes (note that this analysis assumes that the unblocking time is short relative to the total time of observation so that a blocked channel will return to the open state within the time of observation). The predictions of the sequential block model and an alternative model of parallel block are summarized in Table I for ligands with fast and slow unblocking rates and are also described quantitatively in the Appendix.

Tetracaine does not produce a typical sequential block in that the percentage of slow openings does not increase as τ_{b2} decreases with increasing tetracaine concentration. Because of the long blocked times implied by such a scheme, the processes of ligand binding and unbinding and desensitization can modify the actual state of the receptor between the time that tetracaine binds and dissociates. Thus, the data

would effectively rule out the sequential block model for tetracaine in the strictest sense (i.e., the receptor is trapped in the liganded, open, and blocked state until the blocker dissociates) and does not rule out the possibility that the agonist could dissociate or the channel could close before the dissociation of blocker. This suggests that tetracaine is a parallel blocker of the AChR, i.e., the opening and closing of the channel can occur independently of whether or not the blocker is bound. Although the finding that tetracaine is a parallel blocker does not explain why tetracaine exhibits a greater affinity in binding experiments in the absence of agonists, it is consistent with the notion that channel activation is not associated with tetracaine binding.

The effects of both isomers of ANMC are qualitatively consistent with the mechanism of sequential block in that a new component of the closed time distribution is observed and that the ratio of slow to fast bursts increases with increasing ANMC concentration. Two lines of evidence suggest, however, that the data are not quantitatively consistent with the model. The rate of rise of the ratio A_s/A_f can be predicted (see Appendix) and the ratios observed are not within the range predicted by the model (see Fig. 7). Also, the sequential model predicts that the new closed time component, τ_{c3}, should represent blocked times of the channel. This would mean that if t_c for defining a burst duration were set to include most of the τ_{c3} closures, then the time constant for the burst intervals should be correspondingly increased. As described above, this is not the case, which suggests that the channel can open and close while ANMC is bound. Thus, both isomers of ANMC seem to function as parallel blockers, similar to tetracaine. The lack of stereospecific effects of the isomers of ANMC on single channel kinetics (the exception being the increased frequency of fast closures observed with (−)ANMC) is not consistent with the binding (Oswald et al., 1986) data, which predicted a twofold higher affinity for the (−) isomer. On the other hand, the parallel blockade of channel activity is consistent with the small effect of cholinergic agonists on the affinity of both isomers.

The model of parallel block defines those times when the channel's gate is open, and there is no blocker bound, as conductance intervals. A conductance interval begins when either unblocked channels gate to the "open-gated state" or when channels that are in the "open-gated state" dissociate the blocker. The duration of conductance intervals would be exponentially distributed ($\tau_{ci} = 1\ [\alpha + k_{+b}]$), as for any blocked channels. The fact that they may enter the conducting state by more than one kind of transition does not change the kinetics for leaving the state. Clearly some "open-gated states" will not be observed as conductance events at all, especially if the unblocking rate is slow (see Fig. 1). The percentage of the time that the channel is in the open-gated state in the absence of the blocker may be defined as T_{os}. As blocker is added to the bath, the model predicts that the percentage of time in the open-gated state should not change, however, the time spent in conducting intervals (T_{ci}) should decrease. Effectively, every time the channel gates it samples the channel, indicating whether it is blocked or not. In the absence of blocker $T_{ci} = T_{os}$ and in the presence of blocker T_{ci}/T_{os} should give the percentage of the time that the channel is unblocked. The concentration of the blocker at which $T_{ci}/T_{os} = 0.5$ should be the K_d. This analysis requires that the blocker not interfere with agonist binding, it therefore might not be suitable for concentrations of tetracaine over

10 μM, or under other conditions where the blocker is known to affect agonist binding.

Once the model has been used to estimate the K_d of the blocker, the k_{+b} can be calculated from the event duration distribution and k_{-b} can therefore also be estimated. A quantitative test of the model may therefore be made, if an independent estimate of either the K_d or k_{-b} can be obtained. For example, there is an independent way to calculate the K_d for (−)ANMC. By calculating k_{+b} from the event durations ($5.8 \times 10^7\ s^{-1}\ M^{-1}$), and k_{-b} from τ_3 of the closed time distribution ($85\ s^{-1}$), we get an estimate of 1.5 μM for the K_d. Calculating an average T_{os} from the control data we get 0.1108 ± 0.025. The average T_{ci} in the presence of 1 and 2 μM (−)ANMC, were 0.0721 ± 0.035 and 0.0449 ± 0.030, respectively, giving us an average T_{ci} at 2 μM that is somewhat less than half the normal T_{os}, and at 1 μM (−)ANMC the T_{ci} is is perhaps somewhat less than the T_{os}, but still more than half the control value. These values then are consistent with a parallel block of open and closed channels by (−)ANMC and a K_d for the blocker between 1 and 2 μM.

The appearance of an increase in the frequency of fast closures (normalized per second of open time) secondary to effects on burst duration (see Table III), may indicate that these ligands cause more than one form of channel block. In addition to the slow block observed in the low micromolar concentration range, they may also be capable of fast channel block in a higher concentration range, perhaps due to interactions at another channel-associated site. Alternatively, these fast closures might be due to interactions at the agonist binding site. In the case of tetracaine this seemed quite possible since tetracaine is a weak agonist at high concentrations. Agonists appear to produce characteristic nachlage, fast gaps associated with the closed state immediately preceding (the following) channel activation (Colquhoun and Sakmann 1985; Sine and Steinbach 1986*b*; Papke et al., 1988). If at concentrations of tetracaine ≥10 μM, a significant number of events were due to activation of the channel by tetracaine, then the increased frequency of fast closures (τ = 0.6 ms) might represent the characteristic nachlage of tetracaine. To test this possibility some experiments were conducted in a tenfold high concentration of ACh (1 μM vs. the usual 100 nM, data not shown). Under these conditions, far fewer of the currents would be expected to arise from the activation of the channel by tetracaine, yet the frequency of fast closures was unaffected (Papke, 1987). This suggests that these fast closures were not due to tetracaine's interaction with the agonist binding sites.

PCP exhibits the following major effects: (*a*) a shorting of the long burst durations at concentrations below 1 μM, (*b*) a shorting of both long and short burst durations at concentrations above 1 μM, (*c*) an increase in the ratio of the number of short to long bursts at PCP concentrations >1 μM, and (*d*) a lengthening of the long closed duration at concentrations above 1 μM. The decrease in long burst duration in the nanomolar range and a return to control burst durations at 1 μM PCP was also observed by Changeaux et al. (1986) for the AChR of mouse C2 myotubes. Likewise, Aguayo et al. (1986) observed a decrease in the open time of AChRs from rat myoballs at 4 μM PCP.

Taken together these results indicate that PCP can influence the AChR channel lifetime in two concentration ranges, suggesting a complex mechanism of action.

Despite the complexity of the effects observed, several qualitative conclusions can be made. First, at high concentrations, the ratio of the number of slow to fast bursts increases with increasing PCP concentration. This is consistent with the sequential block of open channels, assuming that the unblocking rate is slow relative to the time of observation. This finding is interesting in light of a proposed mechanism for the binding of [^{3}H]PCP to *Torpedo* electroplaque AChR which, in the presence of cholinergic agonists at equilibrium, suggests that the actual binding event occurs when the channel is activated (Oswald et al., 1984). Secondly, the increase in the long closed time constant is consistent with the desensitizing effects of PCP (Karpen et al., 1982; Heidmann et al., 1983; Aguayo et al., 1986). The shortening of the burst duration of nanomolar concentrations, with a possible increase in duration at 1 μM, is difficult to interpret. One possibility is that PCP is capable of both increasing and decreasing the burst duration at distinct sites. Such multiple sites may relate to the multiple sites observed in binding experiments (Heidmann et al., 1983).

In most cases, noncompetitive inhibitors decrease the effect of voltage on burst duration (two exceptions to this generalized effect on voltage dependency may be found in the low concentration ranges of PCP and the (+) isomer of ANMC). The voltage dependency in the presence of ACh alone was extremely complex in that both burst duration and frequency varied with voltage and the effect of voltage on these two parameters varied with ACh concentration. The voltage dependency of blockade by noncompetitive inhibitors could indicate that binding sites for these ligands sense a portion of the membrane field, which would reflect sites of blockade within the channel itself. Alternatively, the inhibitors may modify the normal voltage dependency of the burst duration and frequency of opening observed in the absence of blockers.

In conclusion, these experiments have examined the mechanism of functional inhibition of the nicotinic AChR by noncompetitive antagonists. Three major classes of effects have been observed: (*a*) a block of the channel consistent with a sequential mechanism in the presence of high concentrations of PCP, (*b*) a parallel block by tetracaine and ANMC, in which current is blocked by the antagonist and the channel may close while the blocker is bound, and (*c*) a stabilization of the open channel state by PCP at ~1 μM. These findings are in general agreement with binding studies that suggest that these compounds can have multiple effects which are expressed through multiple binding sites on the ACh receptor.

APPENDIX

Given the simple sequential model for channel blockade shown in scheme 2, the number of openings per burst is given by $1/(1+xk_{b/\alpha})$, where x is the concentration of blocker, k_b is the blocking rate, and α is the closing rate of the channel in the absence of blocker (Colquhoun and Hawkes, 1983). The ratio of "slow" openings per burst to "fast" openings per burst is then given by:

$$\frac{1+\dfrac{xk_b}{\alpha_s}}{1+\dfrac{xk_b}{\alpha_f}}$$

By defining ρ as α_f/α_s, the ratio of slow events to fast events (A_s/A_f) in the presence of blocker is given by:

$$\frac{A_s}{A_f} = \frac{A_{s'}}{A_{f'}}\left[\frac{\frac{1}{\tau_{b2}} + xk_b}{\frac{1}{\tau_{b2'}} + \frac{xk_b}{\rho}}\right]$$

The blocking rate is the slope of the plot of the closing rate vs. the concentration of blocker and is a second order rate constant. ρ and the ratio of slow to fast events in the absence of blocker A_s'/A_f') are determined from the open time distribution in the absence of blocker.

We wish to thank Drs. Glenn Millhauser, Greg Weiland, Dan Wetzel, and Linda Nowak as well as Barbara Coleman for helpful discussions. We also thank Dr. Bruce Land and the Section of Neurobiology of Behavior at Cornell for the loan of equipment.

This work was supported by grants from the Muscular Dystrophy Association and the National Institutes of Health (1 R01 NS 18660-04 NEUB) to R. E. Oswald; additionally, R. L. Papke was supported by an NIH predoctoral training grant (5 T32 GM 07469) to the Graduate Field of Neurobiology and Behavior at Cornell.

Original version received 9 April 1988 and accepted version received 19 October 1988.

REFERENCES

Aguayo, L. G., B. Pazhenchevsky, J. W. Daly, and E. X. Albuquerque. 1981. The ionic channel of the acetylcholine receptor: regulation by sites outside and inside the cell member which are sensitive to quarternary ligands. *Molecular Pharmacolog.* 20:345–355.

Aguayo, L. G., B. Witkop, and E. X. Albuquerque. 1986. Voltage and time dependent effects of phencyclidine on the end-plate current arise from open and closed channel blockage. *Proceedings of the National Academy of Sciences.* 83:3523–3527.

Aracava, Y., S. R. Ikeda, J. W. Daly, N. Brookes, and E. X. Albuquerque. 1984. Interactions of bupivacaine with ionic channels of the nicotinic receptor. *Molecular Pharmacology.* 26:303–313.

Brisson, A., and P. N. T. Unwin. 1985. Quaternary structure of the acetylcholine receptor. *Nature.* 315:474–477.

Caceci, M. S. and W. P. Cacheris. 1984. Fitting curves to data: the simplex algorithm is the answer. *Byte.* 9:340–362.

Carp, J. S., R. S. Aronstam, B. Witkop, and E. X. Albuquerque. 1983. Electrophysiological and biochemical enhancement of desensitization by phenothiazine neuroleptics. *Proceedings of the National Academy of Sciences.* 80:310–314.

Changeux, J. P. 1981. The acetylcholine receptor: an allosteric membrane protein. *Harvey Lectures.* 75:85–254.

Changeux, J. P., C. Pinset, and A. Ribera. 1986. Effects of chlorpromazine and phencyclidine on mouse C_2 acetylcholine receptor kinets. *Journal of Physiology.* 378:497–513.

Cohen, J. B., N. D. Boyd, A. Y. Jeng, D. C. Medysnski, R. R. Neubig, P. St. John, and N. S. Shera. 1980. Permeability control by *Torpedo* acetylcholine receptors. *In* Psychopharmacology and Biochemistry of Neutrotransmitter Receptors. H. Yamamura, R. Olsen, and E. Usdin, editors. Elsevier North Holland, Amsterdam. 47–62.

Coleman, B. A., L. Michel, and R. E. Oswald. 1987. Interaction of a benzomorphan opiate with acetylcholinesterase and the nicotinic acetylcholine receptor. *Molecular Pharmacology.* 32:456–462.

Colquhoun, D., and A. G. Hawkes. 1983. The principles of the stochastic interpretation of ion-channel mechanisms. *In* Single Channel Recording. B. Sakmann and E. Neher, editors. Plenum Publishing Corp., New York. 135–175.

Colquhoun, D., and B. Sakmann. 1985. Fast events in single-channel currents activated by acetylcholine and its analogues at frog muscle end-plates. *Journal of Physiology.* 369:501–557.

Colquhoun, D., and F. J. Sigworth. 1983. Fitting and statistical analysis of single channel records. *In* Single Channel Recording. B. Sakmann and E. Neher, editors. Plenum Publishing Corp. New York. 191–264.

Cos, R. N., R. R. J. Kaldany, M. DiPaola, and A. Karlin. 1985. Time-resolved photolabeling by quinacrine azide on a noncompetitive inhibitor site of the nicotinic acetylcholine receptor in a transient, agonist induced state. *Journal of Biological Chemistry.* 260:7186–7193.

Gage, P. 1976. Generation of end-plate potentials. *Physiology Reviews.* 56:177–247.

Gage, P., R. McBurney, and G. Schneider. 1975. Effects of some alphatic alcohols on the conductance change caused by a quantum of acetylcholine at the toad end-plate. *Journal of Physiology.* 244:409–429.

Giraudat, J., M. Dennis, T. Heidmann, J. P. Changeux, R. Bisson, C. Montecucco, F. Kotozyba-Hilbert, M. Goeldner, C. Hirth, and J. Y. Chang. 1986. Tertiary structure of the nicotinic acetylcholine receptor probe by photolabeling and protein chemistry. *In* Nicotinic Acetylcholine Receptor: Structure and Function. A. Maelicke, editor. Springer-Verlag, Berlin. 103–114.

Hamill, O. P., A. Marty, E. Neher, B. Sakmann, and F. J. Sigworth. 1981. Improved patch-clamp techniques for high resolution current recording from cells and cell-free membrane patches. *Pflügers Archiv.* 391:85–100.

Heidmann, T., and J. P. Changeux. 1979. Fast kinetic studies on the allosteric interactions between acetylcholine receptors and local anesthetic binding sites. *European Journal of Biochemistry.* 94:255–279.

Heidmann, T., R. E. Oswald, and J. P. Changeux. 1983. Multiple sites of action for noncompetitive blockers of acetylcholine receptor rich membrane fragments from *Torpedo marmorata. Biochemistry.* 22:3112–3127.

Jackson, M. B., B. S. Wong, C. E. Morris, H. Lecar and C. N. Christian 1983. Successive openings of the same acetylcholine receptor are correlated in open time. *Biophysical Journal.* 42:109–114.

Karpen, J. W., H. Aoshima, L. G. Abood, and G. P. Hess. 1982. Cocaine and phencyclidine inhibition of the acetylcholine receptor: analysis of the mechanisms of action based on measurements of ion flux in the millisecond-to-minute time region. *Proceedings of the National Academy of Sciences.* 79:2509–2513.

Labarca, P., M. S. Montal, J. M. Lindstrom, and M. Montal. 1985. The occurrence of long openings in the purified cholinergic receptor channel increase with acetylcholine concentration. *Journal of Neuroscience.* 5:3409–3413.

Lambert, J. J., N. N. Durant, and E. G. Henderson. 1983. Drug induced modification of ionic conductance at the neuromuscular junction. *Annual Review of Pharmacology and Toxicology.* 23:505–539.

Neher, E. 1983. The charge carried by single channel currents of rat cultured muscle cells in the presence of local anaesthetics. *Journal of Physiology.* 339:663–678.

Neher, E., and J. H. Steinbach. 1978. Local anaesthetics transiently block current through single acetylcholine receptor channels. *Journal of Physiology.* 277:153–176.

Olsen, E., L. Glaser, J. P. Merlie, R. Sebanne, and J. Lindstrom. 1983. Regulation of surface expression of acetylcholine receptors in response to serum and cell growth in the BC_3H-1 muscle cell line. *Journal of Biological Chemistry.* 258:13946–13953.

Oswald, R. E., M. J. Bamberger, and J. T. McLaughlin. 1984. Mechanism of phencyclidine binding to the acetylcholine receptor from *Torpedo* electroplaque. *Molecular Pharmacology.* 25:360–368.

Oswald, R. E. and J. P. Changeaux. 1981. Ultraviolet light-induced labeling by noncompetitive blockers of the acetylcholine receptor from *Torpedo marmorata. Proceedings of the National Academy of Sciences.* 78:3925–3929.

Oswald, R. E., L. Michel, and J. Bigelow. 1986. Mechanism of binding of a benzomorphan opiate to the acetylcholine receptor from *Torpedo* electroplaque. *Molecular Pharmacology.* 29:179–187.

Papke, R. L. 1987. The gating of single channel currents through the nicotinic acetylcholine receptors of BC_3H-1 cells: effects of agonists and allosteric ligands. Ph.D. Thesis, Cornell University.

Papke R. L., G. Millhauser, Z. Lieberman, and R. E. Oswald. 1988. Relationships of agonist properties to the single channel kinetics of nicotinic acetylcholine receptors. *Biophysical Journal.* 53:1–12.

Papke R. L., and R. E. Oswald, 1986. Effects of allosteric ligands on the gating of single channel currents in BC_3H-1 cells. In Nicotinic Acetylcholine Receptor: Structure and Function. A. Maelicke, editor. Springer-Verlag, Berlin. 243–257.

Sakmann, B., J. Patlak, and E. Neher. 1980. Single acetylcholine activated channels show burst kinetics in presence of desensitizing concentrations of agonist. *Nature.* 286:71–73.

Sheridan, R. E. 1986. Intracellular calcium activates a nonselective cation channel in BC_3H-1 cells. *Neuroscience Abstracts.* 328:18. (Abstr.)

Sigworth, F. J., and S. M. Sine. 1987. Data transformation for improved display and fitting of single channel dwell time histograms. *Biophysical Journal.* 52:1047–1054.

Sine, S. M., and J. H. Steinbach. 1984. Activation of a nicotinic acetylcholine receptor. *Biophysical Journal.* 45:175–185.

Sine, S. M., and J. H. Steinbach. 1986*a*. Acetylcholine receptor activation by a site-selective ligand. *Journal of Physiology.* 370:357–379.

Sine, S. M., and J. H. Steinbach. 1986*b*. Activation of acetylcholine receptors on clonal mammalian BC_3H-1 cells by low concentrations of agonist. *Journal of Physiology.* 373:129–162.

Sine, S. M., and J. H. Steinbach. 1987. Activation of acetylcholine receptors on clonal mammalian BC_3H-1 cells by high concentrations of agonist. *Journal of Physiology.* 385:325–359.

Sine, S. M., and P. Taylor. 1982. Local anesthetics and histrionicotoxin are allosteric inhibitors of the acetylcholine receptor. *Journal of Biological Chemistry.* 257:8106–8114.

Spivak, C. E., M. A. Maleque, A. C. Oliveira, L. M. Masukawa, T. Tokuyama, J. W. Daly, and E. X. Albuquerque. 1982. Actions of the histrionicotoxins at the ion channel of the nicotinic acetylcholine receptor and at the voltage-sensitive ion channels of muscle membranes. *Molecular Pharmacology.* 21:351–361.

Strnad, N. P., and J. P. Cohen. 1983. Tetracaine binding to *Torpedo* post-synaptic membranes. *Neuroscience Abstracts.* 9:160. (Abstr.)

Takeda, K., and A. Trautmann. 1984. A patch clamp study of the partial agonist actions of tubocurarine on rat myotubes. *Journal of Physiology.* 349:353–374.